JACS
JOURNAL OF THE AMERICAN CHEMICAL SOCIETY
Communication
Cite This: J. Am. Chem. Soc. XXXX, XXX, XXX−XXX
pubs.acs.org/JACS

Programming DNA Tube Circumference by Tile Offset Connection

Yingwei Zhang,*[,†] Xianhui Chen,[†] Guangjie Kang,[†] Ruizi Peng,[‡,§] Victor Pan,[§] Ranjani Sundaresan,[§] Pengfei Wang,*[,∥] and Yonggang Ke*[,§,⊥]

[†]State Key Laboratory of Chemical Resource Engineering, College of Materials Science and Engineering, Beijing University of Chemical Technology, Beijing 100082, China

[‡]Molecular Science and Biomedicine Laboratory, State Key Laboratory of Chemo/Bio-Sensing and Chemometrics, College of Chemistry and Chemical Engineering, College of Life Sciences, and Aptamer Engineering Center of Hunan Province, Hunan University, Changsha, Hunan 410082, China

[§]Wallace H. Coulter Department of Biomedical Engineering, Georgia Institute of Technology and Emory University, Atlanta, Georgia 30322, United States

[∥]Institute of Molecular Medicine, Renji Hospital, School of Medicine, Shanghai Jiao Tong University, Shanghai 200127, China

[⊥]Department of Chemistry, Emory University, Atlanta, Georgia 30322, United States

Supporting Information

ABSTRACT: DNA tubes with prescribed circumferences are appealing for numerous multidisciplinary applications. The DNA single-stranded tiles (SSTs) assembly method has demonstrated an unprecedented capability for programming the circumferences of DNA tubes in a modular fashion. Nevertheless, a distinct set of SSTs is typically required to assemble DNA tube of a specific circumference, with wider tubes requiring higher numbers of tiles of unique sequences, which not only increases the expense and design complexity but also hampers the assembly yield. Herein, we introduce "offset connection" to circumvent such challenges in conventional SST tube assembly. In this new connection scheme, the boundary SST tiles in an SST array are designed to connect in an offset manner. To compensate for the offset, the SST array has to grow wider until the array can close to form a wide tube with a tolerable degree of twist. Using this strategy, we have successfully assembled DNA tubes with prescribed circumferences consisting of 8, 12, 14, 16, 20, 24, 28, 32, 36, 42, 56, or 70 helices from two distinct sets of SSTs composed of 19×4 or 19×14 tiles.

Structural DNA nanotechnology represents one of the most robust and versatile molecular self-assembly techniques at the nanoscale and has demonstrated promising applications in a large diversity of fields.[1] Among various DNA structures, DNA tubes have become increasingly appealing for a variety of applications including nanofabrication,[2−7] drug delivery,[8,9] connecting molecular landmarks,[10] and nanoreactors.[11,12]

Precise control of the circumferential geometry of DNA tubes is critical to the aforementioned applications. Several self-assembly strategies have been developed for the fabrication of DNA tubes with prescribed circumference. For instance, the circumferential tube geometry may be encoded into the basic tiles for tube assembly. Using this strategy, DNA tubes comprising three, six, and eight helices have been assembled.[13−16] DNA origami is another powerful approach capable of fabricating tubes of arbitrary circumferential geometry under precise control.[11,17−20] There are also reports of using circular DNA templates as rigid motifs or a small number of synthetically modified/unmodified strands for constructing tubes with controlled diameters and geometries.[21−25] These methods, however, require circumference-specific design of distinct building blocks which often have complicated molecular structures and tedious/error-prone design processes. A modular strategy was developed by Yin et al. whereby single-stranded tiles (SSTs) of unique sequences were programmed to form DNA lattices of prescribed width.[26] The connection between boundary tiles of the lattices led to the formation of tubular structures with monodisperse circumferences of four, five, six, seven, eight, 10, or 20 helices. Using this modular method, one can fabricate DNA tubes with defined circumferences by programming each specific set of tiles involved for assembly (Figure 1a).

Herein, we introduced a new design feature—"offset connection"—into the conventional SST strategy to further expand its modularity by assembling DNA tubes of different defined circumferences from the same basic set of DNA tiles (Figure 1b). For instance, we designed an SST array containing 19×4 tiles—each tile being 42 nucleotides (nt) in length. Unlike in a canonical SST tube, where upper boundary tiles bind to lower boundary tiles of exactly the same x coordinates, offset-connection design programs upper boundary tiles along the x-axis to bind to the lower boundary tiles with a p-tile offset (p = 1, 2, ... 9 for the 19×4-tile array). Such offset connections would prohibit the formation of a four-helix tube, as a large degree of twist of the array is required for a direct closure. Instead, in order to compensate the offset connection, the array would prefer to repetitively grow along the y-axis until a favorable connection of tolerable twist is reached. For example, a three-tile offset design of 19×4 tiles requires six repeats before a favorable closure can be realized to form a 6×4-helix tube (Figure 1b, Figure S1).

Received: August 18, 2019
Published: December 3, 2019

DOI: 10.1021/jacs.9b08921
J. Am. Chem. Soc. XXXX, XXX, XXX−XXX

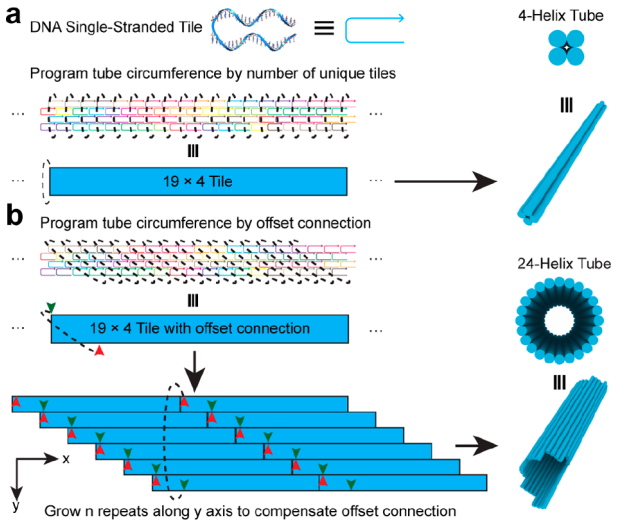

Figure 1. Programming SST DNA tube circumference by offset connection. (a) Conventional single-stranded DNA tile design programs tube circumference by controlling the number of unique tiles along the rolling direction for tube formation. For instance, a 19×4-tile array assembles into a four-helix tube. (b) Programing tube circumference by connecting tiles via offset connections. Due to the offsets, multiple 19×4-tile arrays would grow in the *y*-axis direction before forming a closed tube to compensate the offset.

By programming the number of offsets in the 19×4 tile array, DNA tubes of *n*×4-helix (n = 1−9) circumference may be assembled, as illustrated in Figure 2a. The results show that the offset-connection tubes can tolerate small degrees of twist. We defined the twist of a tube by using a twist angle (θ), which is calculated by counting the number (m) of mismatched tiles between the corresponding two boundaries of DNA lattice after growing n repeats along the *y*-axis (more details are given in Figures S1 and S2). Before carefully analyzing the experimental results, we calculated all possible twist angles θ in each offset-connection design (Table S1). For the 2−9-tile offset-connection designs, the most favorable connections for tube closure (highlighted in red in Table S1) all have one-tile mismatch tolerance (m = 1) after growing n repeats along the *y*-axis, corresponding to twist angles ranging from 5.66° to 24.05°. In contrast, for the one-tile offset-connection design, the calculation provided a relatively large twist angle of 41.75°. We prepared all the 0−9 offset-connection samples via a one-pot isothermal annealing process at the optimized temperature (Figure S3). Atomic force microscopy (AFM) images and measurements confirmed the successful fabrication of tubes in 2−9-tile offset-connection designs, with the tube circumference being fairly uniform for each design (Figure 2b, Figure S4). This suggests that the experimental results matched well with the theoretical predictions, demonstrating that 2−9-tile offset-connection designs with relatively small twist angles ($\theta \leq 24.05°$) could lead to the formation of tubes with a series of prescribed circumferences after the same 19×4-tile array grew n repeats along the *y*-axis. However, the large twist angle of 41.75° in the one-tile offset connection appeared to have prevented the tube formation. A large number n of repeats along the *y*-axis is required to reduce the twist angle, which might be too kinetically unfavorable (Table S1). Herein, we constructed a series of monodisperse DNA tubes with eight different circumferences consisting of 8, 12, 16, 20, 24, 28, 32, and 36 helices by simply programming varied offset

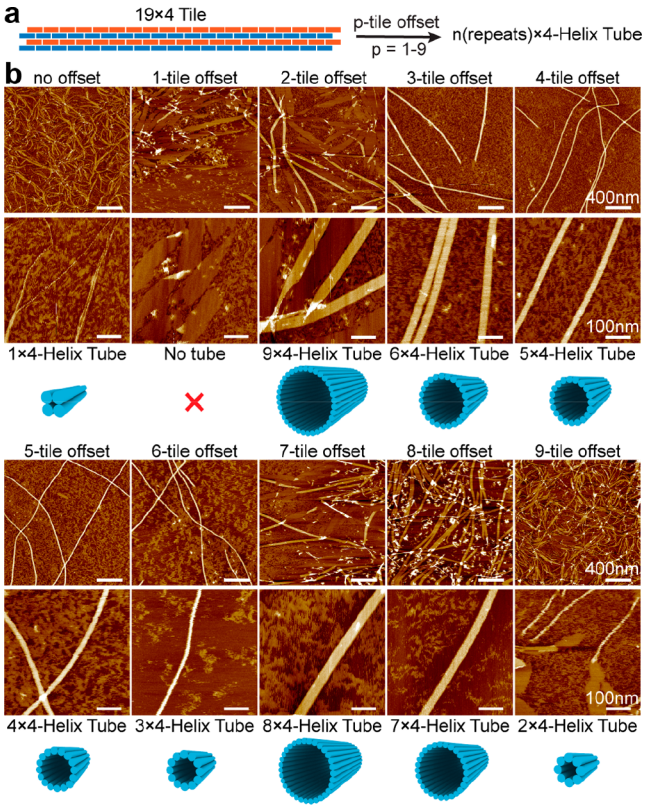

Figure 2. DNA tubes of programmable circumference assembled from 19×4-tile arrays with varied offset-connection designs. (a) Programming circumference of tubes assembled from 19×4-tiles array with *p*-tile offset-connection designs (p = 1−9). (b) AFM images of tubes with varied circumferences and the corresponding *n*×4-helix models (n = 1−9).

connections on boundary tiles based on the same 19×4 tile array. It is worth noting that the measured circumferences of tubes were a bit larger than the calculated values, which can be attributed to the flattening and stretching of the SST tubes on the mica surface (Figure S4).

We also measured the length of these tubes along with assembly yields, which suggests that fewer repeats (n) and smaller twist angle θ led to the formation of DNA tubes with higher yields and longer length. For instance, three-, four-, five-, six-, and eight-tile offset designs with repeat number $n \leq 7$ and twist angle $\theta \leq 16.57°$ (Table S1) all produced monodisperse tubes with length greater than 3 μm or up to 10 μm (Figure S4c), whereas the nine-tile offset design with larger twist angle θ = 24.05° only resulted in the formation of ∼1 μm long tubes, with many open 2D arrays observed. The two- and seven-tile offset designs required large numbers of repeats ($n \geq 8$) to grow into tubes. Hence, these two designs presented lower yields and shorter tubes of ∼3 μm.

To validate the generality of the offset-connection strategy, we further tested it on a larger 19×14-tile array (Figure 3a). Based on the observations from the 19×4-tile array, we anticipated the highly favorable tube formation might contain a one-tile mismatch (labeled in blue in Table S2). We then experimentally assembled these designs using the optimized isothermal annealing protocol (Figure S5). However, no tubes were observed, except for the one-tile and nine-tile offset designs (Figure S6). We hypothesized that the 19×14-tile array may have substantial intrinsic twist due to its larger width,

DOI: 10.1021/jacs.9b08921
J. Am. Chem. Soc. XXXX, XXX, XXX−XXX

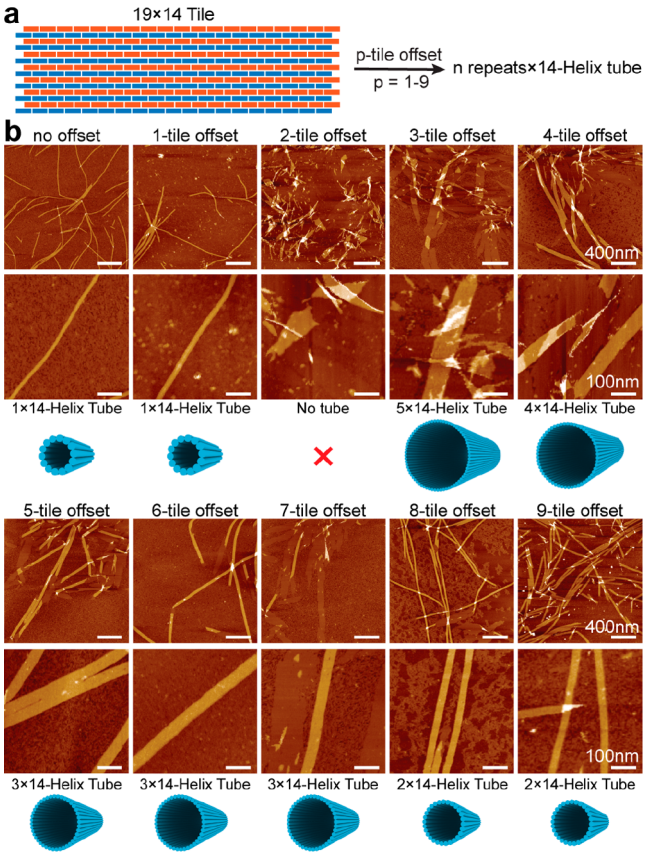

Figure 3. DNA tubes of programmable circumference assembled from 19×14-tile arrays with varied offset-connection designs. (a) Programming circumference of tubes assembled from 19×14-tile array with *p*-tile offset designs (p = 1−9). (b) AFM images of tubes with varied circumferences after introducing the flexible 2T spacer between helixes and the corresponding model of n×14 helix (n = 1−5).

which may hinder the closure of the DNA array to form tubes. Therefore, we added a 2-thymine (2T) flexible spacer into the middle point (at the crossover) of every other row of SST tiles in the 19×14-tile array, to increase the flexibility of the array and facilitate tube closure. Monodisperse tubes with different circumferences were formed (Figure 3b), except for the two-tile offset design, since it requires too many repeats to achieve a relatively small twist angle (Table S2). However, for those successfully assembled tubes, the numbers of mismatched tiles (labeled in red in Table S2 and Figure S7) increased to more than one mismatch, probably due to the increased flexibility induced by the 2T spacer.

We conducted detailed AFM imaging characterizations of the assembled tubes (Figure 3b, Figure S8). The measured widths of these tubes were in good agreement with our anticipation that eight- and nine-tile offset designs yielded 2×14-helix tubes; five-, six-, and seven-tile offset designs produced 3×14-helix tubes; four-tile offset design led to 4×14-helix tubes; and three-tile offset design assembled 5×14-helix tubes. All the calculated twist angles requiring compensation before tube closure in these samples were smaller than 20.93°, which is similar to our previous twist angle results based on the 19×4-tile model. Meanwhile, the two-tile offset design suffered from insufficient growth along the *y*-axis to achieve a tolerable twist angle, resulting in unclosed ribbons. As for the length and assembly yields of these tubes, they obey rules similar to those derived from 19×4-tile tubes—namely that smaller repeating number n, smaller mismatched tiles number m, and smaller twist angle θ all favor the formation of DNA tubes with higher yields and longer length (Figure S8b). For instance, four-, six-, eight-, and nine-tile offset-connection designs produced high tube yields, with the majority of tubes longer than 1 μm.

In summary, we have applied a versatile "offset-connection" strategy to program the circumferences of a series of DNA tubes starting from the same basic SST arrays. The specific offset-connection design provides the driving force for the growing and broadening of the SST arrays along the *y*-axis, and then the synergistic effects of the tolerable twist after growing n repeats along the *y*-axis and the flexibility of the whole DNA structure determine when a favorable binding between the two corresponding boundary tiles occurs for tube formation. Therefore, this offset-connection strategy provides us a modular programming method for preparing a series of DNA tubes with varied circumferences by engineering different offset connections between two boundaries. Using this strategy, we successfully constructed a series of DNA tubes with monodisperse circumferences consisting of 8, 12, 14, 16, 20, 24, 28, 32, 36, 42, 56, or 70 helices from two distinct sets of SSTs comprising 19×4 or 19×14 tiles. The repetitive growth based on the same SST core array and the modular programming of the boundary tiles for a series of offset connections lowered the expense and the design complexity, making it a convenient and low-cost strategy. We believe this offset-connection strategy holds great promise in DNA tube-based templated nanofabrication for sophisticated structures and devices.

■ ASSOCIATED CONTENT

Supporting Information

The Supporting Information is available free of charge at https://pubs.acs.org/doi/10.1021/jacs.9b08921.

Experimental details, extra experimental data, DNA sequences, and DNA strands diagram (PDF)

■ AUTHOR INFORMATION

Corresponding Authors

*zhangyw@mail.buct.edu.cn
*pengfei.wang@sjtu.edu.cn
*yonggang.ke@emory.edu

ORCID

Yingwei Zhang: 0000-0001-8586-864X
Pengfei Wang: 0000-0002-3125-763X
Yonggang Ke: 0000-0003-1673-2153

Notes

The authors declare no competing financial interest.

■ ACKNOWLEDGMENTS

Y.Z. thanks the Natural Science Foundation of China (grants 51672022, 51302010) for support. Y.K. acknowledges NSF grants DMR-1654485 and ECCS-1807568, NIH grant 1R21AI135753-01, and Semiconductor Research Corporation (SRC) grant 2836.002. The AFM images were collected on an atomic force microscope supported by grants GM084070 and 3R01GM084070-07S1 to L.F.

DOI: 10.1021/jacs.9b08921
J. Am. Chem. Soc. XXXX, XXX, XXX−XXX

REFERENCES

(1) Seeman, N. C.; Sleiman, H. F. DNA Nanotechnology. *Nat. Rev. Mater.* **2018**, *3*, 17068.
(2) Zhang, G.; Surwade, S. P.; Zhou, F.; Liu, H. DNA Nanostructure Meets Nanofabrication. *Chem. Soc. Rev.* **2013**, *42*, 2488−2496.
(3) Yan, H.; Park, S. H.; Finkelstein, G.; Reif, J. H.; LaBean, T. H. DNA-templated Self-assembly of Protein Arrays and Highly Conductive Nanowires. *Science* **2003**, *301*, 1882−1884.
(4) Park, S. H.; Barish, R.; Li, H.; Reif, J. H.; Finkelstein, G.; Yan, H.; Labean, T. H. Three-helix Bundle DNA Tiles Self-assemble into 2D Lattice or 1D Templates for Silver Nanowires. *Nano Lett.* **2005**, *5*, 693−696.
(5) Lin, C.; Ke, Y.; Liu, Y.; Mertig, M.; Gu, J.; Yan, H. Functional DNA Nanotube Arrays: Bottom-up Meets Top-down. *Angew. Chem., Int. Ed.* **2007**, *46*, 6089−6092.
(6) Shen, X.; Song, C.; Wang, J.; Shi, D.; Wang, Z.; Liu, N.; Ding, B. Rolling Up Gold Nanoparticle-Dressed DNA Origami into Three-Dimensional Plasmonic Chiral Nanostructures. *J. Am. Chem. Soc.* **2012**, *134*, 146−149.
(7) Douglas, S. M.; Chou, J. J.; Shih, W. M. DNA-nanotube-induced Alignment of Membrane Proteins for NMR Structure Determination. *Proc. Natl. Acad. Sci. U. S. A.* **2007**, *104*, 6644−6648.
(8) Ko, S.; Liu, H.; Chen, Y.; Mao, C. DNA Nanotubes as Combinatorial Vehicles for Cellular Delivery. *Biomacromolecules* **2008**, *9*, 3039−3043.
(9) Lo, P. K.; Karam, P.; Aldaye, F. A.; McLaughlin, C. K.; Hamblin, G. D.; Cosa, G.; Sleiman, H. F. Loading and Selective Release of Cargo in DNA Nanotubes with Longitudinal Variation. *Nat. Chem.* **2010**, *2*, 319−328.
(10) Mohammed, A. M.; Šulc, P.; Zenk, J.; Schulman, R. Self-assembling DNA Nanotubes to Connect Molecular Landmarks. *Nat. Nanotechnol.* **2017**, *12*, 312−316.
(11) Fu, Y.; Zeng, D.; Chao, J.; Jin, Y.; Zhang, Z.; Liu, H.; Li, D.; Ma, H.; Huang, Q.; Gothelf, K. V.; Fan, C. Single-Step Rapid Assembly of DNA Origami Nanostructures for Addressable Nanoscale Bioreactors. *J. Am. Chem. Soc.* **2013**, *135*, 696−702.
(12) Linko, V.; Eerikäinen, M.; Kostiainen, M. A. A Modular DNA Origami-based Enzyme Cascade Nanoreactor. *Chem. Commun.* **2015**, *51*, 5351−5354.
(13) Mathieu, F.; Liao, S.; Kopatsch, J.; Wang, T.; Mao, C.; Seeman, N. C. Six-helix Bundles Designed from DNA. *Nano Lett.* **2005**, *5*, 661−665.
(14) Park, S. H.; Barish, R.; Li, H.; Reif, J. H.; Finkelstein, G.; Yan, H.; LaBean, T. H. Three-Helix Bundle DNA Tiles Self-Assemble into 2D Lattice or 1D Templates for Silver Nanowires. *Nano Lett.* **2005**, *5*, 693−696.
(15) Wei, B.; Mi, Y. A New Triple Crossover Triangle (TXT) Motif for DNA Self-Assembly. *Biomacromolecules* **2005**, *6*, 2528−2532.
(16) Kuzuya, A.; Wang, R.; Sha, R.; Seeman, N. C. Six-helix and Eight-helix DNA Nanotubes Assembled from Half-tubes. *Nano Lett.* **2007**, *7*, 1757−1763.
(17) Chen, H.; Weng, T.-W.; Riccitelli, M. M.; Cui, Y.; Irudayaraj, J.; Choi, J. H. Understanding the Mechanical Properties of DNA Origami Tiles and Controlling the Kinetics of Their Folding and Unfolding Reconfiguration. *J. Am. Chem. Soc.* **2014**, *136*, 6995−7005.
(18) Benn, F.; Haley, N. E. C.; Lucas, A. E.; Silvester, E.; Helmi, S.; Schreiber, R.; Bath, J.; Turberfield, A. J. Chiral DNA Origami Nanotubes with Well-Defined and Addressable Inside and Outside Surfaces. *Angew. Chem., Int. Ed.* **2018**, *57*, 7687−7690.
(19) Dietz, H.; Douglas, S. M.; Shih, W. M. Folding DNA into twisted and curved nanoscale shapes. *Science* **2009**, *325*, 725−730.
(20) Mohammed, A. M.; Schulman, R. Directing Self-Assembly of DNA Nanotubes Using Programmable Seeds. *Nano Lett.* **2013**, *13*, 4006−4013.
(21) Zheng, H.; Xiao, M.; Yan, Q.; Ma, Y.; Xiao, S.-J. Small Circular DNA Molecules Act as Rigid Motifs to Build DNA Nanotubes. *J. Am. Chem. Soc.* **2014**, *136*, 10194−10197.
(22) Aldaye, F. A.; Lo, P. K.; Karam, P.; McLaughlin, C. K.; Cosa, G.; Sleiman, H. F. Modular Construction of DNA Nanotubes of Tunable Geometry and Single- or Double-stranded Character. *Nat. Nanotechnol.* **2009**, *4*, 349−352.
(23) Hamblin, G. D.; Carneiro, K. M. M.; Fakhoury, J. F.; Bujold, K. E.; Sleiman, H. F. Rolling Circle Amplification-Templated DNA Nanotubes Show Increased Stability and Cell Penetration Ability. *J. Am. Chem. Soc.* **2012**, *134*, 2888−2891.
(24) Hamblin, G. D.; Hariri, A. A.; Carneiro, K. M. M.; Lau, K. L.; Cosa, G.; Sleiman, H. F. Simple Design for DNA Nanotubes from a Minimal Set of Unmodified Strands: Rapid, Room-Temperature Assembly and Readily Tunable Structure. *ACS Nano* **2013**, *7*, 3022−3028.
(25) Rahbani, J. F.; Hariri, A. A.; Cosa, G.; Sleiman, H. F. Dynamic DNA Nanotubes: Reversible Switching between Single and Double-Stranded Forms, and Effect of Base Deletions. *ACS Nano* **2015**, *9*, 11898−11908.
(26) Yin, P.; Hariadi, R. F.; Sahu, S.; Choi, H. M. T.; Park, S. H.; LaBean, T. H.; Reif, J. H. Programming DNA Tube Circumferences. *Science* **2008**, *321*, 824−826.

DOI: 10.1021/jacs.9b08921
J. Am. Chem. Soc. XXXX, XXX, XXX−XXX